Highlights of Spanish Astrophysics VII, Proceedings of the X Scientific Meeting of the Spanish Astronomical Society held on July 9 - 13, 2012, in Valencia, Spain. J. C. Guirado, L. M. Lara, V. Quilis, and J. Gorgas (eds.)

Evolution of the bar pattern speed with redshift

I. Pérez[1,2], J. A. L. Aguerri[3,4], and J. Méndez-Abreu[3,4]

[1] Dpto. de Física Teórica y del Cosmos, University of Granada, Facultad de Ciencias (Edificio Mecenas), 18071-Granada, Spain
[2] Instituto Carlos I de Física Teórica y Computación
[3] Instituto de Astrofísica de Canarias, C/ Vía Láctea s/n, 38200 La Laguna, Spain
[4] Departamento de Astrofísica, Universidad de La Laguna, C/ Astrofísico Francisco Sánchez, 38205 La Laguna, Spain

Abstract

In a recent published study we have analysed the evolution of the bar pattern speed with redshift using morphological measurements of a sample of low–inclination ringed galaxies from the SDSS and the COSMOS survey. In this paper we summarise the results obtained in that work. The sample covers a redshift range $0 < z < 0.8$. We have obtained morphological ratios between the deprojected outer ring radius ($R_{\rm ring}$) and the bar size ($R_{\rm bar}$). This quantity is related to the parameter $\mathcal{R} = R_{\rm CR}/R_{\rm bar}$ used for classifiying bars in slow and fast rotators, and allows us to investigate possible differences with redshift. We do not see any change of the R parameter with redshift. These results are compatible with most of the sample ($\sim 70\%$) being fast-rotators and with no evolution of either the pattern speed or the bar size with redshift.

1 Introduction

The bar pattern speed, $\Omega_{\rm b}$, is one of the main kinematic observables in barred galaxies. It describes the dynamics of the bar and determines the position of the resonances in the disc. It is most usefully parametrised by a distance-independent parameter $\mathcal{R} = R_{\rm CR}/R_{\rm bar}$, where $R_{\rm CR}$ is the Lagrangian/corotation radius, where the gravitational and centrifugal forces cancel out in the rest frame of the bar, and $R_{\rm bar}$ is the bar semi-major axis. Therefore, bars that end near corotation ($1 < \mathcal{R} < 1.4$) are considered to be fast, while shorter bars ($\mathcal{R} > 1.4$) are commonly called slow. If $\mathcal{R} < 1.0$, orbits are elongated perpendicular to the bar, and self-consistent bars cannot exist in this regime [10]. The most reliable method for obtaining the location of corotation was that proposed by [31] (hereafter TW method). However, long integration times are required in medium-size telescopes to reach the high signal-to-noise

ratio required to apply the TW method. This limits its application to a small number of candidates. Despite the difficulties in obtaining bar pattern speeds, a reasonable number of nearby galaxies have been investigated [22, 14, 2, 12, 11], finding that all bars end near corotation. Some indirect ways to derive the bar pattern speed include methods based on numerical modelling: [15, 21, 20, 32, 24, 33] and then matching numerical experiments with the observed velocity fields; or by matching numerical simulations to the galaxy morphology [19, 17, 20, 1, 26]. Other indirect methods to derive the bar pattern speed include identifying morphological or kinematic features with resonances: using a variety of features [16, 4]; rings as resonance indicators [7, 9]; phase-shift between the potential and density wave patterns [34].

The technique to determine the bar pattern speed based on connecting the location of rings to orbital resonances was introduced by [7]. It is based on the theoretical work presented by Schwarz in a series of papers [28, 29, 30], showing how these ring structures appear near the dynamical Lindblad resonances due to a bar-like perturbation. To directly apply this method to find the specific value of the pattern speed, not only the location of the ring and the association to a resonance is required, but some kinematic information is also needed. However, we can use the $\mathcal{R}$ parametrisation of the bar introduced previously, and determine the ratio between the outer ring radius (linked to the outer Lindblad resonance, OLR) and the bar length. In this way, we can indirectly determine, not the pattern speed, but whether the bars measured are in the slow or fast regime.

The bar parameters discussed above have been analysed only for local galaxy samples. There are no previous studies in the literature about the evolution of the length, strength and pattern speed of bars with redshift. We present here a summary of the work published in [25] of the the first observational study on the dynamical evolution of bars with redshift. Our approach to quantifying the dynamical state of the bars in our sample of ringed galaxies is based on the measurements of both the bar and ring radius as explained above to obtain an estimation of $\mathcal{R}$. We refer the reader to [25] for more details on the results, methodology and analysis.

2 Sample selection and morphological measurements

The galaxy samples studied in [25] were extracted from two different surveys: low-redshift galaxies were taken from the Sloan Digital Sky Survey (SDSS; $0.01 < z < 0.04$), and high-redshift galaxies were selected from COSMOS ($0.125 < z < 0.75$). The details of the sample selection are given in [25]. We obtained a total of 18 barred galaxies with suitable outer ring features from the SDSS and the high-redshift sample consists of 26 galaxies.

2.1 Outer ring morphological classification

The ring morphological classification used in this study is based on the work of [8]. They divided the outer rings into three main morphological classes resembling the rings developed in numerical simulations near the OLR (see [28]). The first class, called R'_1, is characterised

by a 180° winding of the spiral arms with respect to the ends of a bar. The second type is known as an R'_2 ring. It is defined by a 270° winding of the outer arms with respect to the bar ends, so that in two opposing quadrants the arm pattern is doubled. The R'_1 and R'_2 morphologies were predicted by [28] as the kind of patterns that would be expected near the OLR in a barred galaxy. The third class is referred to in [8] as the $R_1R'_2$ morphology, where the outer arms break not from the ends of the bar, but from an R'_1-type ring. [9] derived the distribution of intrinsic axis ratios for the outer rings using the Catalog of Southern Ringed Galaxies. They found that outer rings present in barred galaxies are intrinsically elliptical with an axis ratio $\sim 0.82 \pm 0.07$, and that the intrinsic ellipticity varies from the R'_1 ($\sim 0.74 \pm 0.08$) to the R'_2 ($\sim 0.87 \pm 0.08$). We decided to remove the R'_1 type of rings from our samples, and keep only the R'_2 types since they are intrinsically rounder. In fact, their intrinsic shape is very similar to that of typical discs [18, 27].

2.2 Outer ring radius and bar size definition

The sample measurements were derived by using the ellipticity and position angle radial profiles extracted from the symmetrised images. A detailed explanation on the ellipse fitting and deprojection method used is given in [25].

In the ring region, we expect that the ellipticity and position angle radial profiles will remain constant because of the stellar orbits in the ring. Therefore, we identifed the region of the profile where the ring is present and we measured the ring radius as the position where the ellipticity and position angle become constants. The error in the ring radius was calculated by comparing the estimated ring radius with the radius at which the ellipticity varies by more than three times the standard deviation of the disc ellipticity.

Different methods have been used to measure the bar length based on the ellipticity and position angle radial profiles (see [5, 23]). However, the solution is always ambiguous and it can lead to misleading results. To remove these uncertainties we decided to measure the bar length as the midpoint between the radius of the maximum and minimum ellipticity in the fitting.

3 Results and discussion

Most galaxy inclinations lie below $i < 40°$. The bar size range, using the maximum ellipticity, covers 2.5 to 6.3 kpc. Most of the bars in the local Universe (about 70%, see [3]) are within this bar size range. Similar values of the bar size range are found for our high-redshift galaxies. The mean bar radius of our low- and high-redshift galaxies are 4.5 ± 1.04 and 3.5 ± 1.33 kpc, respectively. This means that within the errors both galaxy samples have similar bars according to their lengths and they are similar also to local samples of barred galaxies (see [3]). The average bar size, using the minimum ellipticity, for our low- and high-redshift galaxies are also similar: 5.9 ± 1.43 and 5.3 ± 1.70 kpc, respectively. Thus, both samples of galaxies show similar bar sizes independent of the method used for determining the bar length.

We determined the strength of the bars for the low- and high-redshift galaxies by using the maximum ellipticity of the bar (see [3]). Both samples cover the same range of bar strengths. Thus, the mean values of the bar strength of our low- and high-redshift samples are 0.20 ± 0.07, and 0.17 ± 0.05. These values are similar to the mean strength of bars in the local Universe (0.20 ± 0.07; see [3]). We can conclude that according to the size and strength of the bars, our low- and high-redshift galaxy samples have similar bars as those found in a complete local sample of barred galaxies (see [3]).

To determine whether our galaxies are in the *fast* or *slow* range, we defined the ratio $\mathcal{R}_{\rm ring} = R_{\rm ring}/R_{\rm bar}$, where $R_{\rm ring}$ is the ring radius and $R_{\rm bar}$, is the bar semi-major axis, as characterised in Sect. 2.2. Because we cover this ratio for galaxies with redshifts between $0 < z < 0.8$, we can study possible changes of this ratio with redshift. Figure 1 shows the distribution of ring radii ($R_{\rm ring}$) versus the bar semi-major axis ($R_{\rm bar}$) for the whole sample. We considered a fast bar to be those bars for which the $R_{\rm CR}/R_{\rm bar}$ ratio lies between 1.0 and 1.4. This ratio is plotted in Fig. 1 for both values and is calculated using linear resonance theory and a flat rotation curve ([6]). In this case the position of the OLR (i.e., the ring radius) and the CR are related in the following way:

$$\left(\frac{R_{\rm ring}}{R_{\rm CR}}\right)^{\delta} = 1 + \left(1 - \frac{1}{2}\delta\right)^{1/2}, \qquad (1)$$

where δ lies between 0.7 and 1.0 for early-type discs (see [6]). We assumed $\delta = 1.0$ in Fig. 1 for simplicity, but this choice does not alter the results. It is clear from Fig. 1 that all galaxies, independent of their redshift bin, fall into the fast-bar category.

A detailed discussion on the different caveats that could affect our results are given in [25]. None of the discussed problems seem to change the conclusions and results presented.

We found that the bar pattern speed does not seem to change with redshift and that all bars are compatible with being fast bars.

If the bars analysed are long-lasting, their size and bar strength have not significantly changed in time. The fact that, independent of the redshift, the bars are fast rotators and their size has not significantly changed in time could also have strong implications for bar evolution models that mostly predict a bar growth with time.

We have presented the first time that the pattern speed evolution has been investigated from the observational point of view. The results presented in [25] place strong constraints on the bar evolution models.

Acknowledgments

We thank the organizers for a great conference and a fantastic time in Valencia. I.P. was supported by the Spanish Ministry of Science and Innovation (MICINN) (via grants AYA2010-21322-C03-02, AYA2010-21322-C03-03, AYA2007-67625-C02-02 and Consolider-Ingenio CSD2010-00064) and by the Junta de Andalucía (FQM-108). JALA and JMA were supported by the projects AYA2010-21887-C04-04 and by the Consolider-Ingenio 2010 Program grant CSD2006-00070.

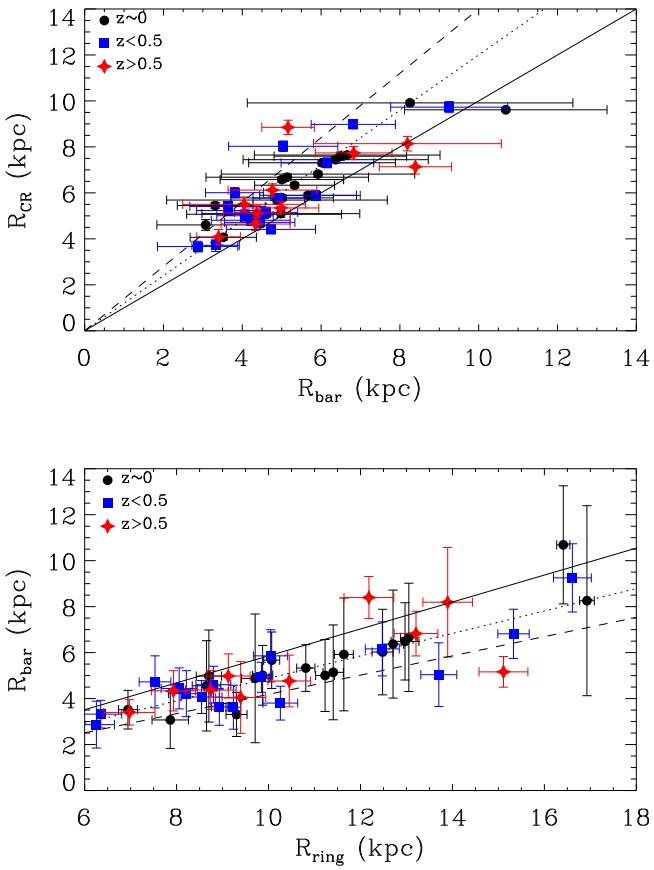

Figure 1: *Top panel*: bar semi-major axis versus corotation radius for the high- and low-redshift sample. The sample was divided into three redshift bins; $z \approx 0$ (solid black circles), $z < 0.5$ (solid blue squares), and $z > 0.5$ (solid red stars). The solid, dotted and dashed lines represent the values, from linear theory, of $\mathcal{R} = R_{\rm CR}/R_{\rm bar} = 1.0, 1.2$ and 1.4, respectively. This range corresponds to what is considered in the literature as fast bars. *Bottom panel*: outer ring radius versus bar semi-major axes radius for the high- and low-redshift sample, the symbols and lines are the same as those represented in the top panel. Notice that all galaxies, regardless of their redshift, clearly fall into the 'fast-bar' region. Figure taken from [25].

References

[1] Aguerri, J. A. L., Hunter, J. H., Prieto, M., et al. 2001, A&A, 373, 786

[2] Aguerri, J. A. L., Debattista, V. P., & Corsini, E. M. 2003, MNRAS, 338, 465

[3] Aguerri, J. A. L., Méndez-Abreu, J., & Corsini, E. M. 2009, A&A, 495, 491

[4] Athanassoula, E. 1992, MNRAS, 259, 345

[5] Athanassoula, E. & Misiriotis, A. 2002, MNRAS, 330, 35

[6] Athanassoula, E., Bosma, A., Creze, M., & Schwarz, M. P. 1982, A&A, 107, 101

[7] Buta, R. 1986, ApJS, 61, 609

[8] Buta, R. & Crocker, D. A. 1991, AJ, 102, 1715

[9] Buta, R., van Driel, W., Braine, J., et al. 1995, ApJ, 450, 593

[10] Contopoulos, G. 1980, A&A, 81, 198

[11] Corsini, E. M. 2011, Memorie della Societa Astronomica Italiana Supplementi, 18, 23

[12] Corsini, E. M., Aguerri, J. A. L., Debattista, V. P., et al. 2007, ApJ, 659, L121

[13] Debattista, V. P. & Sellwood, J. A. 2000, ApJ, 543, 704

[14] Debattista, V. P., Corsini, E. M., & Aguerri, J. A. L. 2002, MNRAS, 332, 65

[15] Duval, M. F. & Athanassoula, E. 1983, A&A, 121, 297

[16] Elmegreen, B. G. & Elmegreen, D. M. 1990, ApJ, 355, 52

[17] England, M. N. 1989, ApJ, 344, 669

[18] Fasano, G., Amico, P., Bertola, F., Vio, R., & Zeilinger, W. W. 1993, MNRAS, 262, 109

[19] Hunter, J. H., Jr., England, M. N., Gottesman, S. T., Ball, R., & Huntley, J. M. 1988, ApJ, 324, 721

[20] Laine, S., Shlosman, I., & Heller, C. H. 1998, MNRAS, 297, 1052

[21] Lindblad, P. A. B., Lindblad, P. O., & Athanassoula, E. 1996, A&A, 313, 65

[22] Merrifield, M. R. & Kuijken, K. 1995, MNRAS, 274, 933

[23] Michel-Dansac, L. & Wozniak, H. 2006, A&A, 452, 97

[24] Pérez, I., Fux, R., & Freeman, K. 2004, A&A, 424, 799

[25] Pérez, I., Aguerri, J. A. L., & Méndez-Abreu, J. 2012, A&A, 540, A103

[26] Rautiainen, P., Salo, H., & Laurikainen, E. 2005, ApJ, 631, L129

[27] Ryden, B. S. 2004, ApJ, 601, 214

[28] Schwarz, M. P. 1981, ApJ, 247, 77

[29] Schwarz, M. P. 1984, A&A, 133, 222

[30] Schwarz, M. P. 1984, MNRAS, 209, 93

[31] Tremaine, S. & Weinberg, M. D. 1984, ApJ, 282, L5

[32] Weiner, B. J., Sellwood, J. A., & Williams, T. B. 2001, ApJ, 546, 931

[33] Zánmar Sánchez, R., Sellwood, J. A., Weiner, B. J., & Williams, T. B. 2008, ApJ, 674, 797

[34] Zhang, X. & Buta, R. J. 2007, AJ, 133, 2584